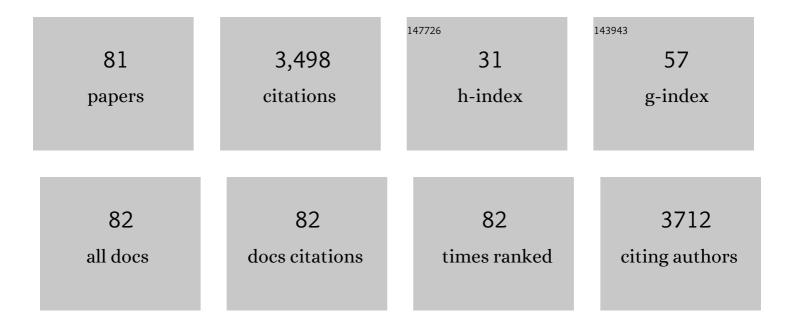
Chechia Hu

List of Publications by Year in descending order

Source: https://exaly.com/author-pdf/2285228/publications.pdf Version: 2024-02-01



Снеснил Ни

#	Article	IF	CITATIONS
1	Ultrafine cobalt nanoparticle-embedded leaf-like hollow N-doped carbon as an enhanced catalyst for activating monopersulfate to degrade phenol. Journal of Colloid and Interface Science, 2022, 606, 929-940.	5.0	24
2	Adsorption kinetics of methyl blue using metal-modified barium lanthanum titanate as an effective absorbent. Materials Chemistry and Physics, 2022, 276, 125363.	2.0	10
3	Broccoli-like CeO2 with Hierarchical/Porous Structures, and promoted oxygen vacancy as an enhanced catalyst for catalytic diesel soot elimination. Separation and Purification Technology, 2022, 281, 119867.	3.9	15
4	Synergistic effect of KCl mixing and melamine/urea mixture in the synthesis of g-C3N4 for photocatalytic removal of tetracycline. Journal of Industrial and Engineering Chemistry, 2022, 107, 118-125.	2.9	18
5	Nanoneedle-Assembled Copper/Cobalt sulfides on nickel foam as an enhanced 3D hierarchical catalyst to activate monopersulfate for Rhodamine b degradation. Journal of Colloid and Interface Science, 2022, 613, 168-181.	5.0	16
6	Synthesis and applications of carbon nitride (CN) family with different carbon to nitrogen ratio. Carbon, 2022, 188, 482-491.	5.4	22
7	Detection of Fe3+ and Hg2+ ions through photoluminescence quenching of carbon dots derived from urea and bitter tea oil residue. Spectrochimica Acta - Part A: Molecular and Biomolecular Spectroscopy, 2022, 272, 120963.	2.0	7
8	HNb3O8/g-C3N4 nanosheet composite membranes with two-dimensional heterostructured nanochannels achieve enhanced water permeance and photocatalytic activity. Chemical Engineering Journal, 2022, 442, 136254.	6.6	22
9	Ag-modified TiO2/SiO2/Fe3O4 sphere with core-shell structure for photo-assisted reduction of 4-nitrophenol. Environmental Research, 2022, 214, 113690.	3.7	19
10	Gel-like Ag-Dicyandiamide Metal–Organic Supramolecular Network-Derived g-C ₃ N ₄ for Photocatalytic Hydrogen Generation. ACS Sustainable Chemistry and Engineering, 2022, 10, 8360-8369.	3.2	14
11	Copper sulfides based photocatalysts for degradation of environmental pollution hazards: A review on the recent catalyst design concepts and future perspectives. Surfaces and Interfaces, 2022, 33, 102182.	1.5	29
12	Boosting photoassisted activity for catalytic oxidation of benzoic acid and reduction of 4-nitrophenol with Ag-supported Fe3O4 aerogel. Chemical Engineering Journal, 2021, 405, 126641.	6.6	20
13	Cobalt ferrite nanoparticle-loaded nitrogen-doped carbon sponge as a magnetic 3D heterogeneous catalyst for monopersulfate-based oxidation of salicylic acid. Chemosphere, 2021, 267, 128906.	4.2	29
14	Lanthanum nanocluster/ZIF-8 for boosting catalytic CO ₂ /glycerol conversion using MgCO ₃ as a dehydrating agent. Journal of Materials Chemistry A, 2021, 9, 7048-7058.	5.2	16
15	The roles of metal species supported on Fe ₃ O ₄ aerogel for photoassisted 4-nitrophenol reduction and benzoic acid oxidation. Catalysis Science and Technology, 2021, 11, 3447-3455.	2.1	3
16	Hydroxylation and sodium intercalation on g-C3N4 for photocatalytic removal of gaseous formaldehyde. Carbon, 2021, 175, 467-477.	5.4	68
17	Self-assembly L-cysteine based 2D g-C3N4 nanoflakes for light-dependent degradation of rhodamine B and tetracycline through photocatalysis. Journal of the Taiwan Institute of Chemical Engineers, 2021, , .	2.7	21
18	Production of glycerol carbonate from carboxylation of glycerol with CO2 using ZIF-67 as a catalyst. Chemical Engineering Science, 2021, 235, 116451.	1.9	34

#	Article	IF	CITATIONS
19	Influence of Phosphorus Doping on Triazole-Based g-C ₃ N ₅ Nanosheets for Enhanced Photoelectrochemical and Photocatalytic Performance. ACS Applied Materials & Interfaces, 2021, 13, 24907-24915.	4.0	70
20	Photoluminescence quenching of thermally treated waste-derived carbon dots for selective metal ion sensing. Environmental Research, 2021, 197, 111008.	3.7	24
21	MIL-88B(Fe)-coated photocatalytic membrane reactor with highly stable flux and phenol removal efficiency. Chemical Engineering Journal, 2021, 418, 129469.	6.6	41
22	Hierarchical ZIF-decorated nanoflower-covered 3-dimensional foam for enhanced catalytic reduction of nitrogen-containing contaminants. Journal of Colloid and Interface Science, 2021, 602, 95-104.	5.0	19
23	Degradation of an imidazolium-based ionic liquid in water using monopersulfate catalyzed by Dahlia flower-like cobalt oxide. Separation and Purification Technology, 2021, 274, 118668.	3.9	8
24	Insights into the deposition of nanostructured nickel oxides by amino acid chelated Complexes: Benefits of mixed side chains in the formation of nanostructures for Energy-efficient Electrochromic windows. Applied Surface Science, 2021, 568, 150914.	3.1	3
25	Assessing nickel oxide electrocatalysts incorporating diamines and having improved oxygen evolution activity using <i>operando</i> UV/visible and X-ray absorption spectroscopy. Physical Chemistry Chemical Physics, 2021, 23, 23280-23287.	1.3	6
26	Freeze-dried dicyandiamide-derived g-C3N4 as an effective photocatalyst for H2 generation. Journal of the Taiwan Institute of Chemical Engineers, 2021, 129, 128-134.	2.7	21
27	Structural modification of aminoclay for catalytic applications. Chemical Engineering Communications, 2020, 207, 871-886.	1.5	7
28	Graphene oxide-derived carbon-doped SrTiO3 for highly efficient photocatalytic degradation of organic pollutants under visible light irradiation. Chemical Engineering Journal, 2020, 383, 123116.	6.6	78
29	Coordination polymer-derived porous Co3O4 nanosheet as an effective catalyst for activating peroxymonosulfate to degrade sulfosalicylic acid. Applied Surface Science, 2020, 532, 147382.	3.1	29
30	Influence of P,S,O-Doping on g-C3N4 for hydrogel formation and photocatalysis: An experimental and theoretical study. Carbon, 2020, 169, 338-348.	5.4	153
31	Palladium nanoparticles supported on nanosheet-like graphitic carbon nitride for catalytic transfer hydrogenation reaction. Catalysis Science and Technology, 2020, 10, 7883-7893.	2.1	12
32	Selective synthesis of ZIFs from zinc and nickel nitrate solution for photocatalytic H2O2 production. Arabian Journal of Chemistry, 2020, 13, 8301-8308.	2.3	17
33	Boosting photocatalytic H ₂ O ₂ production by coupling of sulfuric acid and 5-sulfosalicylic acid incorporated polyaniline with g-C ₃ N ₄ . Sustainable Energy and Fuels, 2020, 4, 4186-4195.	2.5	14
34	Influence of Photocatalysis on Blood Cell Attachment over Protein-Immobilized Polystyrene Surfaces Modified with a Poly(styrene)- <i>b</i> -Poly(acrylic acid) Copolymer. Langmuir, 2020, 36, 3268-3275.	1.6	4
35	Novel Architecture Titanium Carbide (Ti3C2Tx) MXene Cocatalysts toward Photocatalytic Hydrogen Production: A Mini-Review. Nanomaterials, 2020, 10, 602.	1.9	114
36	Towards artificial photosynthesis: Sustainable hydrogen utilization for photocatalytic reduction of CO2 to high-value renewable fuels. Chemical Engineering Journal, 2020, 402, 126184.	6.6	123

#	Article	IF	CITATIONS
37	Enhanced degradation of 5-sulfosalicylic acid using peroxymonosulfate activated by ordered porous silica-confined Co3O4 prepared via a solvent-free confined space strategy. Separation and Purification Technology, 2020, 249, 116972.	3.9	23
38	Polymeric g-C3N4 Derived from the Mixture of Dicyandiamide and Mushroom Waste for Photocatalytic Degradation of Methyl Blue. Topics in Catalysis, 2020, 63, 1182-1192.	1.3	6
39	Sulfur-doped g-C3N4 nanosheets for photocatalysis: Z-scheme water splitting and decreased biofouling. Journal of Colloid and Interface Science, 2020, 567, 202-212.	5.0	90
40	Mushroom waste-derived g-C3N4 for methyl blue adsorption and cytotoxic test for Chinese hamster ovary cells. Materials Chemistry and Physics, 2020, 244, 122715.	2.0	13
41	De Novo synthesis of platinum-nanoparticle-encapsulated UiO-66-NH2 for photocatalytic thin film fabrication with enhanced performance of phenol degradation. Journal of Hazardous Materials, 2020, 397, 122431.	6.5	44
42	Development of 3-dimensional Co3O4 catalysts with various morphologies for activation of Oxone to degrade 5-sulfosalicylic acid in water. Science of the Total Environment, 2020, 724, 138032.	3.9	20
43	Advances in Designing Au Nanoparticles for Catalytic Epoxidation of Propylene with H2 and O2. Catalysts, 2020, 10, 442.	1.6	18
44	Development of BiOI as an effective photocatalyst for oxygen evolution reaction under simulated solar irradiation. Catalysis Science and Technology, 2020, 10, 3223-3231.	2.1	22
45	Structural, microstructural, electrical, thermal and non-isothermal degradation kinetic studies on technologically important poly(aniline)/CdO nanocomposites. Journal of Sol-Gel Science and Technology, 2019, 91, 611-623.	1.1	6
46	Synergistic Effect of Hydrochloric Acid and Phytic Acid Doping on Polyaniline-Coupled g-C ₃ N ₄ Nanosheets for Photocatalytic Cr(VI) Reduction and Dye Degradation. ACS Applied Materials & Interfaces, 2019, 11, 35702-35712.	4.0	89
47	Photocatalytic Dye and Cr(VI) Degradation Using a Metal-Free Polymeric g-C3N4 Synthesized from Solvent-Treated Urea. Polymers, 2019, 11, 182.	2.0	33
48	Heterostructural design of I-deficient BiOI for photocatalytic decoloration and catalytic CO2 conversion. Catalysis Science and Technology, 2019, 9, 3800-3811.	2.1	21
49	Amine functionalized ZIF-8 as a visible-light-driven photocatalyst for Cr(VI) reduction. Journal of Colloid and Interface Science, 2019, 553, 372-381.	5.0	87
50	Optical, thermal, mechanical properties, and nonâ€isothermal degradation kinetic studies on PVA/CuO nanocomposites. Polymer Composites, 2019, 40, 3737-3748.	2.3	39
51	Phosphorus-doped g-C3N4 integrated photocatalytic membrane reactor for wastewater treatment. Journal of Membrane Science, 2019, 580, 1-11.	4.1	99
52	Microwave plasma torch synthesis of Zn Al oxides as adsorbent and photocatalyst for organic compounds removal. Powder Technology, 2019, 344, 454-462.	2.1	16
53	Decoration of SrTiO3 nanofibers by BiOI for photocatalytic methyl orange degradation under visible light irradiation. Journal of the Taiwan Institute of Chemical Engineers, 2019, 96, 264-272.	2.7	31
54	Recent Developments in Graphitic Carbon Nitride Based Hydrogels as Photocatalysts. ChemSusChem, 2019, 12, 1794-1806.	3.6	87

#	Article	IF	CITATIONS
55	Biofouling mechanism of polysaccharide–protein–humic acid mixtures on polyvinylidene fluoride microfiltration membranes. Journal of the Taiwan Institute of Chemical Engineers, 2019, 94, 2-9.	2.7	6
56	Ag@Sr2TiO4/Bi5O7I Heterostructured Composite for Solar-Driven Photoelectrochemical Analysis. ECS Journal of Solid State Science and Technology, 2018, 7, Q70-Q73.	0.9	2
57	Fabrication of antistatic fibers with core/sheath and segmented-pie configurations. Journal of Industrial Textiles, 2018, 47, 569-586.	1.1	13
58	Yellowish and blue luminescent graphene oxide quantum dots prepared <i>via</i> a microwave-assisted hydrothermal route using H ₂ O ₂ and KMnO ₄ as oxidizing agents. New Journal of Chemistry, 2018, 42, 3999-4007.	1.4	55
59	Phosphorus and sulfur codoped g-C3N4 as an efficient metal-free photocatalyst. Carbon, 2018, 127, 374-383.	5.4	220
60	Ag-Deposited Electrospun SrTiO3 Nanofiber with Enhanced Photocatalytic Activity for Degradation of Methylene Orange. Journal of Nanoscience and Nanotechnology, 2018, 18, 445-450.	0.9	3
61	N-doped NaTaO 3 synthesized from a hydrothermal method for photocatalytic water splitting under visible light irradiation. Journal of Energy Chemistry, 2017, 26, 515-521.	7.1	22
62	Waterborne polyurethane molecular structure designed and its acetic acid and ammonia absorption efficiency. Fibers and Polymers, 2017, 18, 835-841.	1.1	3
63	Influence of solvothermal synthesis on the photocatalytic degradation activity of carbon nitride under visible light irradiation. Chemical Engineering Science, 2017, 167, 1-9.	1.9	35
64	Rapid synthesis of g-C3N4 spheres using microwave-assisted solvothermal method for enhanced photocatalytic activity. Journal of Photochemistry and Photobiology A: Chemistry, 2017, 348, 8-17.	2.0	64
65	Photoluminescence and Photocatalysis of Gallium Oxynitride Synthesized from Nitridation of Ga2O3. ECS Journal of Solid State Science and Technology, 2017, 6, Q3001-Q3006.	0.9	10
66	Heterojunction of n-type Sr 2 TiO 4 with p-type Bi 5 O 7 I with enhanced photocatalytic activity under irradiation of simulated sunlight. Applied Surface Science, 2017, 426, 536-544.	3.1	34
67	Fabrication and characterization of antistatic fiber with segmented pie structure. Textile Reseach Journal, 2016, 86, 1828-1836.	1.1	4
68	Semianalytical solution for powerâ€law polymer solution flow in a converging annular spinneret. AICHE Journal, 2015, 61, 3489-3499.	1.8	6
69	Pyrochlore-like K2Ta2O6 synthesized from different methods as efficient photocatalysts for water splitting. Catalysis Science and Technology, 2013, 3, 1798.	2.1	22
70	Powerâ€law polymer solution flow in a converging annular spinneret: Analytical approximation and numerical computation. AICHE Journal, 2012, 58, 122-131.	1.8	9
71	Efficient water splitting over Na1â^'xKxTaO3 photocatalysts with cubic perovskite structure. Journal of Materials Chemistry, 2011, 21, 3824.	6.7	69
72	Influence of Indium Doping on the Activity of Gallium Oxynitride for Water Splitting under Visible Light Irradiation. Journal of Physical Chemistry C, 2011, 115, 2805-2811.	1.5	31

#	Article	IF	CITATIONS
73	Structural features of p-type semiconducting NiO as a co-catalyst for photocatalytic water splitting. Journal of Catalysis, 2010, 272, 1-8.	3.1	142
74	Gallium Oxynitride Photocatalysts Synthesized from Ga(OH) ₃ for Water Splitting under Visible Light Irradiation. Journal of Physical Chemistry C, 2010, 114, 20100-20106.	1.5	62
75	Structure Characterization and Tuning of Perovskiteâ€Like NaTaO ₃ for Applications in Photoluminescence and Photocatalysis. Journal of the American Ceramic Society, 2009, 92, 460-466.	1.9	88
76	Electrodeposited p-type Cu2O as photocatalyst for H2 evolution from water reduction in the presence of WO3. Solar Energy Materials and Solar Cells, 2008, 92, 1071-1076.	3.0	181
77	Electrodeposited p-type Cu2O for H2 evolution from photoelectrolysis of water under visible light illumination. International Journal of Hydrogen Energy, 2008, 33, 2897-2903.	3.8	203
78	Temperature-Dependent Photoluminescence in NaTaO[sub 3] with Different Crystalline Structures. Electrochemical and Solid-State Letters, 2008, 11, P1.	2.2	35
79	Influence of structural features on the photocatalytic activity of NaTaO3 powders from different synthesis methods. Applied Catalysis A: General, 2007, 331, 44-50.	2.2	163
80	NaTaO3 photocatalysts of different crystalline structures for water splitting into H2 and O2. Applied Physics Letters, 2006, 89, 211904.	1.5	131
81	Preparation and characterization of carbon black/polybutylene terephthalate/polyethylene terephthalate antistatic fiber with sheath–core structure. Journal of the Textile Institute, 0, , 1-9.	1.0	9